Molecular Imaging for the in Vivo Monitoring of Angiogenesis in a Hindlimb Ischemia Animal Model

Konstantia Tsioupinaki[1], Stavros Spiliopoulos[2], Dimitris Karnabatidis[2],George Loudos[3], George C. Nikiforidis[1], George C. Kagadis[1,*]

1. Department of Medical Physics, School of Medicine, University of Patras, Greece.
2. Department of Radiology, School of Medicine, University of Patras, Greece.
3. Department of Biomedical Engineering, Technological Educational Institute of Athens, Greece.

A B S T R A C T

Purpose: Integrin $\alpha_v\beta_3$ is a promising imaging target of angiogenic activity which is up-regulated on activated but not on quiescent endothelial cells. Molecular imaging of $\alpha_v\beta_3$ integrin expression with the aid of a dedicated high resolution gamma camera, is a very sensitive imaging approach for the evaluation of angiogenesis in the rabbit hindlimb ischemia model. Furthermore, in order to evaluate the whole spectrum of endogenous process of collateralization after occlusion of an artery, Digital Subtraction Angiography (DSA) was also used for the visualization of larger collaterals.

Methods: The study included seven New Zealand White rabbits that underwent unilateral percutaneous endovascular embolization of the femoral artery, for the establishment of hindlimb ischemia that triggers the endogenous process of collateralization. The contralateral limb was not embolized and served as a control. The radiotracer that was employed for the angiogenesis imaging, was a $^{99\,m}$Tc labeled cyclic RGD peptide ([c RGDfk-His]-^{99m}Tc) that binds specifically to $\alpha_v\beta_3$ integrin via a three amino acid sequence (Arginine-Glycine-Aspartic acid or RGD). Image acquisition was performed with a high resolution gamma camera and all animals underwent molecular imaging on the 3rd day and the 9th day post-embolization. In all animals DSA was performed on the 9th day post-embolization.

Results: The acquired images demonstrated the retention of the radiotracer at the ischemic tissue is remarkably increased compared to the non-ischemic hindlimb (normal limb) (mean value 16020 ± 2309 vs. 13139 ± 2493 on day 3; p=0.0014 and 21616 ± 2528 vs. 13362 ± 2529 on day 9; p<0.0001, respectively). In addition, radiotracer retention in normal limbs seemeds to be increased at day 9 in normal limbs compared to day 3 (p=0.0112). DSA demonstrated the mean vessel length detected was significantly superior in the normal compared to the ischemic limb at day 9 (mean value 3680 ± 369.8 vs. 2772 ± 267.7; p< 0.0001, respectively).

Conclusion: Angiogenesis was successfully detected using a 99 mTc labeled cyclic RGD peptide molecular imaging technique and was significantly more pronounced in the ischemic compared to normal limbs, both at 3rd and 9th days after embolization. The peak of the phenomenon was detected at 9th days. Finally increased retention of radiotracer in normal limbs at day 9 indicates presence and gradual accumulation of activated endothelium in normal tissues as well.

*** Corresponding Author:**

George C. Kagadis, PhD

Assistant Professor of Medical Physics – Medical Informatics, Department of Medical Physics, School of Medicine, University of Patras, P.O. BOX: 132. 73, GR 265 04, Rion, Greece.

Tel: +30 2610 969146

E-mail: gkagad@gmail.com / George.Kagadis@med.upatras.gr

1. Introduction

Peripheral vascular disease (PVD) is caused by atherosclerotic occlusion of the arteries those supply the lower extremities, resulting in muscle ischemia and inadequate oxygen supplies. The normal mechanism that compensates tissue ischemia encompasses two distinct biological processes that occur in parallel; angiogenesis and arteriogenesis [1]. Angiogenesis is defined as the sprouting of new capillaries whereas arteriogenesis is the formation of collateral arteries by enlargement of preexistent collateral arterioles [2, 3, 4]. Angiogenesis and arteriogenesis are initiated by distinct triggering signals. The driving force for angiogenesis is hypoxia in the surrounding tissue. Due to hypoxia, a transcription factor named hypoxia-inducible factor-1 (HIF-1) is expressed, binds hypoxia response elements (HREs) within the promoters of target genes and activates their transcription [5]. The HIF pathway regulates a host of pro-angiogenic genes including vascular endothelial growth factor (VEGF), angiopoietin-2, Tie2 receptor, platelet-derived growth factor (PDGF), basic fibroblast growth factor (bFGF) and monocyte chemoattractant protein-1 (MCP-1). HIF-regulated pro-angiogenic factors implement the HIF-specific angiogenic cascade by increasing vascular permeability, endothelial cell proliferation, sprouting, migration, adhesion, and tube formation [6].

In contrast, arteriogenesis is induced independently of the presence of hypoxia. After narrowing or occlusion of the lumen of a large artery, the distal arterial blood pressure drops, leading to a pressure gradient along preexistent collateral vessels. As a result, blood flow is redistributed via the pre-existent arterioles which now connect a high-pressure with a low-pressure region. This causes a flow velocity increase and consequently amplified shear stress in the pre-existent collateral vessels. Increased wall shear stress causes a marked activation of the endothelium accompanied with increases in the expression of MCP-1 and of endothelial surface receptors involved in monocyte tethering, rolling and migration [7, 8, 9]. Monocytes adhere to intraluminal surface of vessel wall and migrate to the abluminal space where they transform into macrophages, produce numerous cytokines and growth factors involved in arteriogenesis [10]. These factors include, MCP-1 which induces the attraction of more monocytes to the sites of proliferation, tumor necrosis factor alpha (TNF-α) which provides the inflammatory environment, prerequisite for the collateral vessel development, b-FGF which is a mitogen for both endothelial and smooth muscle cells and

matrix metalloproteinases (MMPs) that remodels the perivascular space and creates an appropriate environment for the expansion of collaterals [11, 12].

Hershey et al. [13] demonstrated a clear temporal dissociation between capillary sprouting and arteriogenesis. According to this study, angiogenesis occurs and is maximized within the first 5 days after femoral artery occlusion in New Zealand White rabbits whereas the growth of angiographically visible collateral vessels takes place after approximately 10 days. Consequently the time course of angiogenesis and arteriogenesis were clearly distinct. Moreover angiogenesis was associated with reduced resting hindlimb blood flow and detectable levels of skeletal muscle VEGF. In contrast, arteriogenesis did not correlate with tissue ischemia or skeletal muscle VEGF content but did exhibit improvement in blood flow reserve.

Experiments were designed in order to in vivo evaluate the whole spectrum of the recovery mechanism following the onset of ischemia. That is, at early time points when capillary sprouts are formed in the hypoxic region distal to the occlusion and at late time points when collateral arteries are formed in the upper thigh proximal to the occlusion. Angiogenesis offers a temporary relief to hypoxia by locally increasing blood perfusion of hypoxic tissue and restoring local oxygen and nutrient supply. Arteriogenesis on the other hand is induced in order to restore functional blood flow circulation of the extremities. Precise evaluation of the normal recovery mechanism with the aid of a noninvasive imaging approach, serves as valuable tool for the assessment of therapeutic stimulation and acceleration of this natural protective mechanism [14]. Molecular imaging of angiogenesis with the aid of a dedicated gamma camera is a highly sensitive imaging approach that enables direct evaluation of primary mediators of angiogenesis [15, 16]. Integrin $\alpha_v\beta_3$ is one of the key molecules during angiogenesis and is highly expressed on the surface of proliferating endothelial cells that migrate to form the capillary sprouts, but not on quiescent ones [17, 18]. Characterization and evaluation of the expression profile of $\alpha_v\beta_3$ and therefore of the angiogenic response is feasible if $\alpha_v\beta_3$ integrin is targeted with a radiolabelled RGD peptide [19]. The RGD sequence is proved to allow high affinity and specific binding to the $\alpha_v\beta_3$ integrin [20, 21]. This experimental protocol was designed to investigate the time course and progress of angiogenesis as detected by the changes in the relative retention of a cyclic RGD peptide labeled with Technetium (^{99m}Tc) in a model of peripheral hindlimb ischemia [22]. The specific RGD peptide [cRGDfk-His] has demonstrated

acceptable labeling, kinetics and blood pool clearance [23]. Digital Subtraction Angiography (DSA) was also used for the visualization of larger collaterals which according to the literature are first detected about 10 days after occlusion [14, 24].

2. Methods

This in vivo experimental protocol was designed to conform to the Guide for the Care and Use of Laboratory Animals (United States National Institutes of Health Publication No. 85-23, revised 1996) and was approved by the Hospital's Scientific and Ethical Committee. The study included seven (n= 7) New Zealand White rabbits (male sex, weight 3.0 – 4.0 kg) that underwent unilateral percutaneous endovascular embolization of the femoral artery. The contralateral limb was not embolized and served as a control. All animals underwent molecular imaging on the 3rd day and the 9th day post-embolization. In all animals (n=7) DSA was performed on the 9th day post-embolization.

2.1. Ischemia Animal Model

For the purpose of our study we used the well-established hindlimb ischemia model of New Zealand White rabbits [14]. All animals were anesthetized using an intramuscular injection of ketamine (50 mg/kg) and xylazine (10 mg/kg) and bilateral hindlimb ischemia was induced in all rabbits with an established endovascular technique of selective intra-arterial coil embolization, using the trans-auricular access as previously described [24, 25]. Initially, access was obtained through the central auricular artery of the animal using a 22G standard intravenous catheter, followed by 2-3 ml of diluted non-ionic iodinated contrast media (Visipaque® 320 mg I/ml, GE Healthcare, Buckinghamshire, United Kingdom) manual infusion as to acquire road map images of the carotid artery and the thoracic aorta. Under road map imaging, a 0.018 inch glide wire (V-18 control wire; Boston Scientific, Natick, MA) was advanced through the carotid artery and the descending thoracic aorta to the abdominal aorta and a 4F × 12 cm 0.018' compatible sheath (Bolton Medical, Villers-les- Nancy, France) was introduced over- the-wire into the external carotid artery to secure the arterial access. In cases in which the guide wire was not advanced from the carotid artery to the descending thoracic, a C1 catheter (Terumo Europe, Leuven, Belgium) was used to enable catheterization. Once the guide wire was advanced into the distal abdominal aorta, a 4F angled glide-catheter was positioned just above the aortic bifurcation, contrast media was infused and road map images of the arterial

bed of both limbs were obtained. Successively, a 0.035' stiff hydrophilic guide wire (Terumo Europe, Leuven, Belgium), was used in order to catheterize the common iliac artery and the 4F catheter was advanced to the distal femoral artery. Intra-arterial embolization was performed initially with a 4/50 mm fibered coil in order to cover the entire femoral artery from its distal end to the origin of the deep femoral artery. Subsequently, the deep femoral artery was selectively catheterized with a micro-catheter (Progreat, Terumo Europe, Leuven, Belgium) and two 3/80 mm spiral coils were positioned through the origin of the deep femoral artery, extending backwards for a few millimetres into the femoral artery. Final angiography was performed with the catheter in the distal aorta five minutes after embolization as to certify the complete occlusion of both deep and superficial femoral arteries. Finally, the sheath was removed and haemostasis was attained by 5 minutes of manual compression at the puncture site, while antibiotic prophylaxis with intramuscular ampicillin C (0.1 mg/kg) was administered [26].

2.2. Molecular Imaging

A ^{99m}Tc labeled cyclic RGD peptide ([c RGDfk-His]-^{99m}Tc) was employed for angiogenesis imaging in the New Zealand White rabbits hindlimb ischemia model. Imaging of $\alpha_v\beta_3$ expression was performed in all animals. Imaging was employed 3 days and 9 days post femoral artery occlusion. Each rabbit was injected intravenously with 200 µl of [c RGDfk-His]$^{-99m}$Tc (0.5 mCi). Consequently dynamic planar imaging was performed using a dedicated gamma camera of 1.5 mm spatial resolution with field of view (FOV) 5 × 10 cm, equipped with a parallel hole collimator and a pixilated NaI(Tl) scintillator. The animals' legs were properly placed on the field of the dedicated gamma camera and were arranged at defined markers to ensure a uniform orientation during image acquisition. All images were digitally stored in a 100 × 50 matrix [22, 27, 28]. Following image acquisition the image integrated intensity value was measured over a specific orthogonal area extending to the area where embolization has been induced. Thus a measure of peptide concentration in the area of interest was obtained and consequently we ended in an indirect measure of angiogenesis induction over that area.

2.3. Intra-Arterial Digital Subtraction Angiography and Image Post-Processing

Digital subtraction angiography (DSA; DVI-S Angiography Unit, Philips, Amsterdam, Netherlands) with an image acquisition protocol of 1 image per second at

40–90 kV, was utilized as an adjunct to molecular imaging for the investigation of limb vascularization and perfusion 9 days after the procedure. Once again using the trans-auricular arterial approach described above, a 4F catheter was advanced 2-3 cm proximal to the abdominal aortic bifurcation and a total volume of 3 ml of the same non-ionic iodinated contrast was infused, at a rate of 1 ml/s, through an automated angiographic injector pump. The hindlimbs of the rabbits were positioned at a distance of 25 cm from the X-ray tube, while the focal spot to intensifier distance was 110 cm [25]. Angiography imaging post-processing was performed with the application of a previously described quantitative analysis of collateral vessels based on the multi-scale structural tensor model [29]. In brief, baseline digital angiographic image was initially smoothened with a 2D Gaussian sigma standard deviation and then the Hessian matrix, also called structural matrix, was produced by the second order Gaussian derivatives of the image. Step-wise multi-scale Eigen-value analysis of the Hessian matrix accomplishes precise extraction and segmentation of the vasculature map within the image. Subsequently, a region-of-interest (ROI) was designed in the area of the medial thigh to comprise the newly developed collaterals. All limbs were processed using the same ROIs in order to reproduce equal sampling areas. Pixel counts normalization against a known size was achieved by using the tip of the 4F angiographic catheter included in the DSA frames. A skeletonization procedure that collapses vessel diameter to one pixel was performed and the selected vessels were measured both with regard to their total vessel area and their length, while the software segmented and quantified collateral vessels with a diameter greater than 500 μm, to focus the study on the process of arteriogenesis and collateralization. Again, the mean intensity was measured as described in the molecular imaging protocol.

2.4. Statistical Analysis

The statistical analysis of all data was performed with the GraphPad PRISM statistical software (version 5; San Diego, California, USA). Data are expressed as mean ± SD. Comparisons between groups were analysed by Student's t-test to determine significant differences. The threshold of statistical significance was set to $p < 0.05$.

3. Results

All animals survived the embolization procedure and follow-up period. Successful molecular and DSA imaging was obtained in all 7 animals (14 limbs) used in our study (Figures 1 & 2). Results showed an increased uptake of the radiotracer at the ischemic hindlimbs, which is more pronounced on day 9 after ischemia induction. The acquired images demonstrated the retention of the radiotracer at the ischemic tissue is remarkably increased compared to the non-ischemic hindlimb (normal limb): 16020 ± 2309 vs. 13139 ± 2493 on day 3; p=0.0014 (paired t-test) and 21616 ± 2528 vs. 13362 ± 2529 on day 9; p<0.0001 (paired t-test; mean radiotracer uptake values are given in arbitrary units), respectively (Figure 3). In addition, radiotracer retention in normal limbs seems to be increased on day 9 in normal limbs compared to day 3 (p=0.0112; paired t-test).

DSA quantification demonstrated the mean vessel length detected was significantly superior in the normal compared to the ischemic limb on day 9; mean value 3680 ± 369.8 pixels vs. 2772 ± 267.7 pixels; p< 0.0001 (paired t-test), respectively as demonstrated in Figure 4. Results of molecular imaging and DSA quantification at day 9 post embolization, in both ischemic and normal hindlimbs are analytically reported in Table 1.

Table 1. Quantitative measures of peptide concentration and DSA measurements on the ROIs (over which quantification took place) of ischemic and non-ischemic limbs on day 9 post ischemia induction.

|	MI		DSA	
	Image Integrated Intensity		Vessel Length in Pixels	
	Ischemic limb	Normal limb	Ischemic limb	Normal limb
1	22506	14304	2915	3820
2	18078	9061	2234	3015
3	25621	15788	3015	4039
4	21987	15399	2980	3980
5	20378	12198	2769	3501
6	19473	11442	2654	3470
7	23269	15339	2834	3932
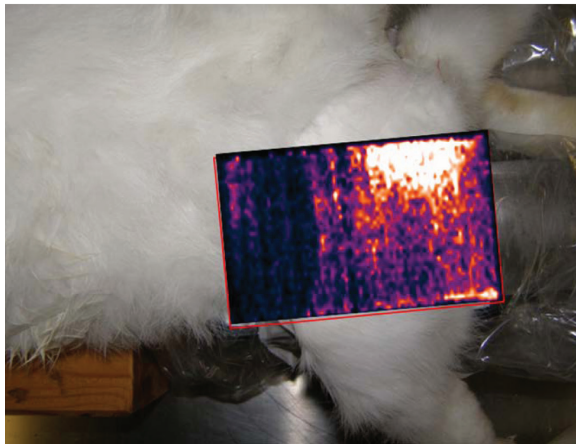
Figure 1. New Zealand White rabbit with the correlated molecular imaging picture of the ischemic hindlimb on day 9 post-embolization.
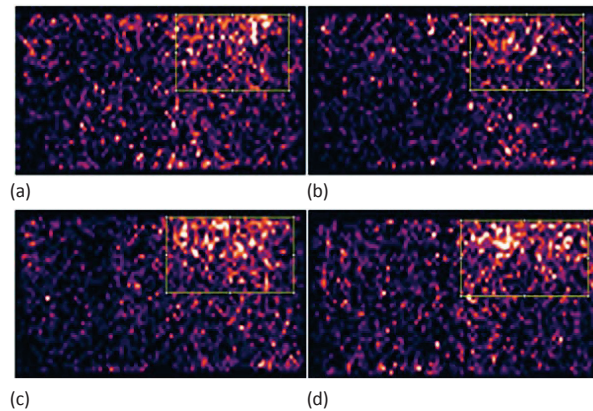
Figure 2. Molecular imaging demonstrating the superior radiotracer uptake in the ischemic (a) and (c) versus the normal (b) and (d) rabbit hindlimb, at 3 (a, b) and 9 (c and d) days post embolization respectively.
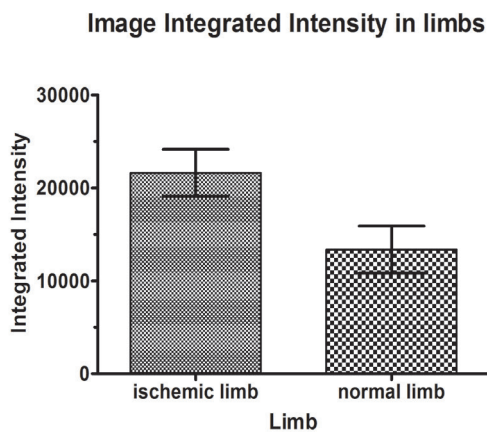
Figure 3. Graphical representation of the mean values of the intensity of the radiotracer detected after molecular imaging, in ischemic versus normal animal hindlimbs.
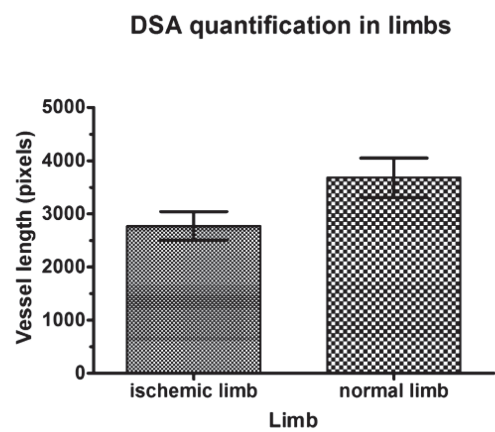
Figure 4. Graphical representation of the mean values of vessel length following quantification of the DSA images, in ischemic versus normal animal hindlimbs.

4. Discussion

In this study we demonstrate the value of imaging the $\alpha_v\beta_3$ integrin expression profile during capillary sprouting in a peripheral hindlimb ischemia model, using a highly sensitive noninvasive radiotracer technique. In order to evaluate the time course of $\alpha_v\beta_3$ expression, images were acquired at different time points after occlusion. The results clearly indicate that there is significant uptake of the radiotracer in the case of ischemic tissue compared to the normal tissue. Moreover focal RGD peptide retention was elevated as early as 3 days after onset of ischemia and peaked at 9 days after occlusion. The fact that radiotracer retention in normal limbs was also increased at day 9 compared to day 3 could be attributed to the presence and gradual accumulation of activated endothelial cells in normal tissues too. In order to evaluate the formation of larger collaterals DSA was performed. Results from the angiographic imaging indicated that large collateral vessels ($> 50 - 100$ μm) were

significantly less in the ischemic compared to normal limbs 9 days after the onset of ischemia. As expected DSA quantification detected significantly superior mean vessel length in normal limbs, demonstrating that although angiogenesis is pronounced in day 9, arteriogenesis is not sufficiently pronounced. However, even at day 9 the development of larger vessels detectable with DSA was evident, demonstrating the phenomenon of arteriogenesis has initiated as reported elsewhere [13].

For the precise evaluation of angiogenic response after onset of ischemia, a radiotracer-based technique has been used in our study as it enables visualization, quantification and characterization of angiogenesis in response to ischemia. Molecular imaging of angiogenesis, utilizing a dedicated gamma camera and a radiotracer that binds to a specific and primary mediator of angiogenesis, is a noninvasive procedure that allows imaging changes in extremity capillary networks. Among the advantages of this method, is the high sensitivity of the imaging modality that enables detection of the radiotracer at very low concentrations within the body, irrespectively of the depth inside the body where it has been accumulated [30, 31]. Moreover this method has the advantage of detecting changes in biological processes at a very early time point as targets are genes and proteins whose expression profile changes a long time before a condition is characterized as pathological.

The molecular target in our experiment is integrin $\alpha_v\beta_3$, which is found in abundance on the surface of proliferating endothelial cells that form capillary sprouts during angiogenesis but not on quiescent ones. Therefore it is considered as a specific marker of ongoing angiogenesis [32]. Integrin $\alpha_v\beta_3$ is a heterodimer trans-membrane receptor that serves as mechanical link between the extracellular proteins and the cytoskeleton inside the cell. The integrin receptor family in mammalians consists of 24 distinct integrins made up of 8 β subunits assorted with 18 α subunits. Ligation of integrins modulates many aspects of cell behavior such as, survival/apoptosis, proliferation, motility, polarity, shape, differentiation and gene expression all of which are central processes in the course of angiogenesis. The molecular pathways that are stimulated by ligation of integrin resemble are connected with those triggered by growth factor receptors such as VEGFR-2 with which specifically $\alpha_v\beta_3$ is closely associated. That means cellular response to growth factors, prerequisite for cellular survival and proliferation, depends on cellular anchorage to extracellular matrix (ECM) components via integrin ligation [33].

Hua et al. [22] studied the time course of $\alpha_v\beta_3$ expression during angiogenesis with the use of high-resolution gamma camera in a murine hindlimb ischemia model and the research indicated that angiogenic process peaks at day 7 after occlusion which is significantly down regulated at day 14 after onset of ischemia. Moreover, the study demonstrated the changes in the expression profile of $\alpha_v\beta_3$ were localized at distal to occlusion regions where angiogenesis evolves and not at proximal to occlusion regions where collateral vessels are formed. Our results seem to be corresponded with those of Hua et al. [22], although this protocol did not include longer term imaging as to detect the time point of angiogenesis down regulation. Further limitations of this protocol are the relatively small number of animals studied, as well as the fact that it did not include pathological specimen correlation with the molecular imaging findings.

Conclusively, according to the specific protocol the angiogenesis was successfully detected using a ^{99m}Tc labeled cyclic RGD peptide molecular imaging technique. Angiogenesis was significantly more pronounced in the ischemic compared to normal limbs, both at day 3 and day 9 after embolization, while the peak of the phenomenon was detected at day 9. Finally, activated endothelium was detected in normal tissues as well as it was indicated by the relative retention of the radiotracer at day 9 at the non-ischemic limbs.

Acknowledgements

References

[1] Heilmann, C., Beyersdorf, F., & Lutter, G. (2002). Collateral growth: cells arrive at the construction site. Cardiovasc Surg, 10(6), 570-578.

[2] Carmeliet, P. (2000). Mechanisms of angiogenesis and arteriogenesis. Nat Med, 6(4), 389-395.

[3] Risau, W. (1997). Mechanisms of angiogenesis. Nature, 386(6626), 671-674.

[4] Schaper, W., & Buschmann, I. (1999). Arteriogenesis, the good and bad of it. Cardiovasc Res, 43(4), 835-837.

[5] Semenza, G. L., & Wang, G. L. (1992). A nuclear factor induced by hypoxia via de novo protein synthesis binds to the human erythropoietin gene enhancer at a site required for transcriptional activation. Mol Cell Biol, 12(12), 5447-5454.

[6] Krock, B. L., Skuli, N., & Simon, M. C. (2011). Hypoxia-induced angiogenesis: good and evil. Genes Cancer, 2(12), 1117-1133.

[7] Gimbrone, M. A., Jr., Nagel, T., & Topper, J. N. (1997). Biomechanical activation: an emerging paradigm in endothelial adhesion biology. J Clin Invest, 99(8), 1809-1813.

[8] Resnick, N., & Gimbrone, M. A., Jr. (1995). Hemodynamic forces are complex regulators of endothelial gene expression. FASEB J, 9(10), 874-882.

[9] Shyy, Y. J., Hsieh, H. J., Usami, S., & Chien, S. (1994). Fluid shear stress induces a biphasic response of human monocyte chemotactic protein 1 gene expression in vascular endothelium. Proc Natl Acad Sci U S A, 91(11), 4678-4682.

[10] Schaper, J., Konig, R., Franz, D., & Schaper, W. (1976). The endothelial surface of growing coronary collateral arteries. Intimal margination and diapedesis of monocytes. A combined SEM and TEM study. Virchows Arch A Pathol Anat Histol, 370(3), 193-205.

[11] Arras, M., Ito, W. D., Scholz, D., Winkler, B., Schaper, J., & Schaper, W. (1998). Monocyte activation in angiogenesis and collateral growth in the rabbit hindlimb. J Clin Invest, 101(1), 40-50.

[12] Arras, M., Strasser, R., Mohri, M., Doll, R., Eckert, P., Schaper, W., et al. (1998). Tumor necrosis factor-alpha is expressed by monocytes/macrophages following cardiac microembolization and is antagonized by cyclosporine. Basic Res Cardiol, 93(2), 97-107.

[13] Hershey, J. C., Baskin, E. P., Glass, J. D., Hartman, H. A., Gilberto, D. B., Rogers, I. T., et al. (2001). Revascularization in the rabbit hindlimb: dissociation between capillary sprouting and arteriogenesis. Cardiovasc Res, 49(3), 618-625.

[14] Katsanos, K., Karnabatidis, D., Diamantopoulos, A., Kagadis, G. C., Ravazoula, P., Nikiforidis, G. C., et al. (2009). Thrombin promotes arteriogenesis and hemodynamic recovery in a rabbit hindlimb ischemia model. J Vasc Surg, 49(4), 1000-1012.

[15] Orbay, H., Hong, H., Zhang, Y., & Cai, W. (2013). PET/SPECT imaging of hindlimb ischemia: focusing on angiogenesis and blood flow. Angiogenesis, 16(2), 279-287.

[16] Stacy, M. R., Maxfield, M. W., & Sinusas, A. J. (2012). Targeted molecular imaging of angiogenesis in PET and SPECT: a review. Yale J Biol Med, 85(1), 75-86.

[17] Horton, M. A. (1997). The alpha v beta 3 integrin "vitronectin receptor". Int J Biochem Cell Biol, 29(5), 721-725.

[18] Beer, A. J., & Schwaiger, M. (2008). Imaging of integrin alphavbeta3 expression. Cancer Metastasis Rev, 27(4), 631-644.

[19] Ruoslahti, E. (1996). RGD and other recognition sequences for integrins. Annu Rev Cell Dev Biol, 12, 697-715.

[20] Morrison, M. S., Davis, J., Ricketts, S. A., Cuthbertson, A., & Mendizabal, M. V. (2003). Monitoring of tumour response to therapy with a novel angiogenesis imaging agent. Mol Imaging, 2, 272.

[21] Tsiapa, I., Loudos, G., Varvarigou, A., Fragogeorgi, E., Psimadas, D., Tsotakos, T., et al. (2013). Biological evaluation of an ornithine-modified (99m)Tc-labeled RGD peptide as an angiogenesis imaging agent. Nucl Med Biol, 40(2), 262-272.

[22] Hua, J., Dobrucki, L. W., Sadeghi, M. M., Zhang, J., Bourke, B. N., Cavaliere, P., et al. (2005). Noninvasive imaging of angiogenesis with a ^{99m}Tc-labeled peptide targeted at alphav-beta3 integrin after murine hindlimb ischemia. Circulation, 111(24), 3255-3260.

[23] Bouziotis, P., Psimadas, D., Fani, M., Gourni, E., Loudos, G., Xanthopoulos, S., et al. (2006). Radiolabeled biomolecules for early cancer detection and therapy via angiogenesis targeting. Nuclear Instruments and Methods in Physics research A, 569, 492-496.

[24] Karnabatidis, D., Katsanos, K., Diamantopoulos, A., Kagadis, G. C., & Siablis, D. (2006). Transauricular arterial or venous access for cardiovascular experimental protocols in animals. J Vasc Interv Radiol, 17(11 Pt 1), 1803-1811.

[25] Karatzas, A., Katsanos, K., Lilis, I., Papadaki, H., Kitrou, P., Lecht, S., et al. (2013). NGF promotes hemodynamic recovery in a rabbit hindlimb ischemic modelthrough trkA- and VEGFR2-dependent pathways. J Cardiovasc Pharmacol, 62(3), 270-7.

[26] Spiliopoulos, S., Diamantopoulos, A., Katsanos, K., Ravazoula, P., Karnabatidis, D., & Siablis, D. (2011). PolarCath cryoplasty enhances smooth muscle cell apoptosis in a rabbit iliac artery model: an experimental in vivo controlled study. Cryobiology, 63(3), 267-272.

[27] Higuchi, T., Wester, H. J., & Schwaiger, M. (2007). Imaging of angiogenesis in cardiology. Eur J Nucl Med Mol Imaging, 34 Suppl 1, S9-19.

[28] Meoli, D. F., Sadeghi, M. M., Krassilnikova, S., Bourke, B. N., Giordano, F. J., Dione, D. P., et al. (2004). Noninvasive imaging of myocardial angiogenesis following experimental myocardial infarction. J Clin Invest, 113(12), 1684-1691.

[29] Kagadis, G. C., Spyridonos, P., Karnabatidis, D., Diamantopoulos, A., Athanasiadis, E., Daskalakis, A., et al. (2008). Computerized analysis of digital subtraction angiography: a tool for quantitative in-vivo vascular imaging. J Digit Imaging, 21(4), 433-445.

[30] Kagadis, G. C., Loudos, G., Katsanos, K., Langer, S. G., & Nikiforidis, G. C. (2010). In vivo small animal imaging: current status and future prospects. Med Phys, 37(12), 6421-6442.

[31] Munley, M. T., Kagadis, G. C., McGee, K. P., Kirov, A. S., Jang, S., Mutic, S., et al. (2013). An introduction to molecular imaging in radiation oncology: A report by the AAPM working group on molecular imaging in Radiation oncology (WGMIR). Med Phys, 40(10), 101501-23.

[32] Morrison, A. R., & Sinusas, A. J. (2010). Advances in radionuclide molecular imaging in myocardial biology. J Nucl Cardiol, 17(1), 116-134.

[33] Hynes, R. O. (2002). Integrins: bidirectional, allosteric signaling machines. Cell, 110(6), 673-687.